Neurobiology of Disease

Neurocytoma Is a Tumor of Adult Neuronal Progenitor Cells

Fraser J. Sim,[1]* H. Michael Keyoung,[2]* James E. Goldman,[3] Dong Kyu Kim,[4] Hee-Won Jung,[4] Neeta S. Roy,[2] and Steven A. Goldman[1,2]

[1]Department of Neurology, University of Rochester Medical Center, Rochester, New York 14642, [2]Department of Neurology, Weill Medical College of Cornell University, New York, New York 10021, [3]Department of Pathology, Columbia University Medical School, New York, New York 10032, and[4]Department of Neurosurgery, Seoul National University, Seoul 110-744, Korea

Central neurocytoma (CN) is a rare periventricular tumor, whose derivation, lineage potential, and molecular regulation have been mostly unexplored. We noted that CN cells exhibited an antigenic profile typical of neuronal progenitor cells *in vivo*, yet *in vitro* generated neurospheres, divided in response to bFGF (basic fibroblast growth factor), activated the neuroepithelial enhancer of the nestin gene, and gave rise to both neuron-like cells and astrocytes. When CN gene expression was compared with that of both normal adult VZ (ventricular zone) and E/nestin:GFP (green fluorescent protein)-sorted native neuronal progenitors, significant overlap was noted. Marker analysis suggested that the gene expression pattern of CN was that of a proneuronal population; glial markers were conspicuously absent, suggesting that the emergence of astroglia from CN occurred only with passage. The expression pattern of CN was distinguished from that of native progenitor cells by a cohort of differentially expressed genes potentially involved in both the oncogenesis and phenotypic restriction of neurocytoma. These included both IGF2 and several components of its signaling pathway, whose sharp overexpression implicated dysregulated autocrine IGF2 signaling in CN oncogenesis. Both receptors and effectors of canonical wnt signaling, as well as GDF8 (growth differentiation factor 8), PDGF-D, and neuregulin, were differentially overexpressed by CN, suggesting that CN is characterized by the concurrent overactivation of these pathways, which may serve to drive neurocytoma expansion while restricting tumor progenitor phenotype. This strategy of comparing the gene expression of tumor cells to that of the purified native progenitors from which they derive may provide a focused approach to identifying transcripts important to stem and progenitor cell oncogenesis.

Key words: **brain tumor; neural stem cell; tumor stem cell; ventricular zone; oncogenomics; expression profile**

Introduction

The ventricular wall of the human forebrain ventricles harbors a persistent pool of neural stem cells that remain mitotic throughout life (Kirschenbaum et al., 1994; Pincus et al., 1997, 1998a; Roy et al., 2000a; Sanai et al., 2004), and retain the capacity to produce both neurons and glia (Gage, 2000; Goldman, 2003). These cells may comprise a major source of tumors of the CNS (Singh et al., 2003, 2004; Sanai et al., 2005), especially in pediatric brain tumors, in which periventricular tumors predominate (Hemmati et al., 2003). The subependyma also appears to include neuronally restricted progeny of the stem cell pool, at least some of which remain mitotically competent while still within the subependymal compartment (Menezes et al., 1995; Roy et al., 2000a). These cells may be prospectively identified and isolated from the adult human brain (Roy et al., 2000a), just as from the brains of lower species. Central neurocytoma (CN) is a rare periventricular neuronal tumor of young adults (Kim et al., 1997; Schild et al., 1997), whose origin, phenotypic potential, and molecular regulation have remained mostly unexplored, despite an extensive literature attesting to its neuronal antigenicity *in vivo* (Patt et al., 1996; Tsuchida et al., 1996), and its production of both neurons and glia in culture (Ishiuchi et al., 1998). Its neuronal phenotype, along with its typical presentation along the lateral ventricular wall, suggests that neurocytoma originates from subependymal neural progenitor cells. It shares this site of origin with tumors such as primitive neuroectodermal and dysplastic neuroepithelial tumors, as well as subependymomas, each of which exhibit periventricular predominance. Unlike other periventricular tumors, however, neurocytoma cells exhibit a primarily neuronal morphology and antigenicity; they express βIII-tubulin, N-CAM (neural cell adhesion molecule), neuron-specific enolase, and synaptophysin (Patt et al., 1996; Tsuchida et al., 1996), prototypic neuronal markers, and present histologically as round-cell tumors, with subependymal neuroblastic morphologies (Akimoto et al., 1995). The characteristic phenotype and ventricular location of these tumors suggested to us that neurocytoma might arise by the transformation of neuronally biased, transit-amplifying progenitor cells of the adult subependyma.

In this set of studies, we compared the lineal relationships and gene expression patterns of central neurocytoma cells to those of native adult human neural progenitor cells. By so doing, we tested the hypothesis that neurocytoma may represent a transformed derivative of neuronal progenitor cells of the adult subependyma.

Received Feb. 23, 2006; revised Aug. 28, 2006; accepted Sept. 17, 2006.

This work was supported by National Institute of Neurological Disorders and Stroke Grant R01NS33106. We thank Drs. Henry Furneaux, Urban Lendahl, and Hideyuki Okano for their gifts of antibodies and Drs. Richard Fraser of Cornell–New York Hospital and Sun-Ha Paek of Seoul National University for providing tissue samples.

*F.J.S. and H.M.K. contributed equally to this work.

Correspondence should be addressed to Dr. Steven A. Goldman, Division of Cell and Gene Therapy, Department of Neurology, University of Rochester Medical Center, 601 Elmwood Avenue/MRBX Box 645, Rochester, NY 14642. E-mail: steven_goldman@urmc.rochester.edu.

DOI:10.1523/JNEUROSCI.0829-06.2006

 0270-6474/06/2612544-12$15.00/0

We found that neurocytoma cells expand as bipotential neuronal-astrocytic progenitor cells *in vitro*, but are strongly biased toward neurogenesis *in vivo*. Molecular profiling of neurocytoma, and the comparison of its expression profile to that of neural progenitors sorted from adult human lateral ventricular wall, indicated substantial overlap of neurocytoma and native progenitor cell gene expression. Nonetheless, neurocytoma could be distinguished from native neural progenitor cells by its selective upregulation of a discrete cohort of functionally related transcripts. Most prominent among these were IGF2 and its downstream signal intermediaries, as well as several wnt pathway members that included Frizzled-1 (FZD1) and T cell transcription factor 4 (TCF4), and a select cohort of ligands that included PDGF-D, neuregulin, and growth differentiation factor 8 (GDF8). These findings suggest a causal relationship between dysregulated IGF2 and wnt signaling with the origin and expansion of neurocytoma from native subependymal progenitor cells. These observations further suggest the usefulness of assessing tumor gene expression patterns by normalizing against those of the native stem and progenitor cells from which those tumors might arise, both as a means of assessing tumor ontogeny, and of identifying specific oncogenic targets for therapeutic intervention.

Materials and Methods

Clinical cases

This study included cell culture, histological, and RNA analyses of 11 pathologically confirmed cases of central neurocytoma. Case 1 was obtained for cell culture after resection at New York Hospital–Cornell, cases 2–7 were assessed histologically on retrospective review of cases identified at Columbia Presbyterian Hospital, and cases 8–11 were identified after resection at the Seoul National University Hospital; the latter were used predominantly for RNA analyses (cases 9–11). All 11 samples were assessed histologically and antigenically. In addition, non-neoplastic control tissues were obtained from four patients at New York Hospital–Cornell, who underwent temporal lobectomy for medication-refractory epilepsy.

Immunostaining

Fresh frozen samples were obtained from surgical samples, cryosectioned at 12 μm, and mounted onto Superfrost slides. From all samples, biopsies were also fixed in formalin and embedded into paraffin, from which 15 μm sections were cut. Representative sections were assessed from each tumor by hematoxylin–eosin, and additional sections were then immunostained for either: synaptophysin [mouse monoclonal antibody (mAb); Chemicon, Temecula, CA], glial fibrillary acidic protein (GFAP) (rabbit polyclonal antibody; Sigma, St. Louis, MO), TuJ-1/βIII tubulin (clone 5G8; Promega, Madison, WI), neurofilament (rabbit polyclonal antibody; Sigma), Hu (mAb 16A11; 25 μg/ml; Dr. H. Furneaux, Memorial Sloan-Kettering Cancer Center, New York, NY), CNPase (2′,3′-cyclic nucleotide 3′-phosphohydrolase) (Chemicon), nestin (rabbit anti-human nestin; Dr. U. Lendahl, Karolinska Institute, Stockholm, Sweden), and musashi (rat anti-musashi mAb 14C1; Dr. H. Okano, Keio University School of Medicine, Tokyo, Japan). To determine the mitotic index, MIB-1 (sheep anti-human Ki-67; Serotec, Indianapolis, IN) was used to identify Ki-67. Secondary antibodies were directly conjugated to FITC or Texas Red.

Cultures were fixed with 4% paraformaldehyde and stained as above for either nestin, musashi, TuJ1/βIII tubulin or Hu, or GFAP. Species and idiotype-specific secondary antibodies were directly conjugated with FITC or Texas Red.

Neurocytoma tissue culture

Resected tumor tissue was collected in Ca/Mg-free HBSS, and then cut into small pieces in PIPES solution (120 mM NaCl, 5 mM KCl, 25 mM glucose, 20 mM PIPES), and prepared as described previously (Roy et al., 2000a,b; Lee et al., 2003). The tissue was then resuspended in DMEM/F-12/N2, containing 5% fetal bovine serum (FBS) (Invitrogen, San Diego, CA), basic fibroblast growth factor (bFGF) (20 ng/ml), and epidermal growth factor (EGF) (10 ng/ml). The cells were plated at 4×10^6 cells $\cdot$ ml^{-1} $\cdot$ well^{-1} into six-well Falcon Primaria plates, precoated with collagen IV (Becton Dickinson, Mountain View, CA) or fibronectin (Sigma), and incubated at 37°C in 5% CO_2. Once 90% confluence was reached, the cells were split and passaged. For generation of neurospheres, the CN cells were plated onto low-cluster plates (Corning, Corning, NY) and cultured under low-adhesive conditions in serum-free DMEM/F-12/N2 supplemented with bFGF (20 ng/ml) and EGF (10 ng/ml).

Isolation of native adult neural progenitor cells

The ventricular zone (VZ) was dissected from four temporal lobectomies resected for medication-refractory epilepsy, as described previously (Roy et al., 2000a,b). These samples of adult VZ were either directly frozen in liquid nitrogen for subsequent RNA extraction, or dissociated for progenitor isolation via adenoviral E/nestin:green fluorescent protein (GFP)-based fluorescence-activated cell sorting (FACS), also as described previously (Keyoung et al., 2001). In brief, the papain-dissociated cells were raised in DMEM/F-12/N2 with 20 ng/ml FGF2 for 5–7 d, infected with adenoviral E/nestin:EGFP (enhanced GFP) at 5 multiplicities of infection, and then sorted within a week thereafter for GFP$^+$ cells. Fluorescence-activated cell sorting was accomplished using a FACSVantage (Becton Dickinson), at 1000–3000 cells/s, with a purification-mode algorithm. E/nestin:*lacZ* transfected cells were used to set the background fluorescence; a false-positive rate of 0.1–0.3% was accepted so as to ensure adequate yield.

[^{3}H]Thymidine incorporation assay

First-passage CN cells were cultured in DMEM/F-12/N2 with 5% FBS in 24-well plates, and then switched to 20 ng/ml bFGF or 10 ng/ml EGF in DMEM/F-12/N2 with 1% FBS, for 1 week in the presence of 3.5 μCi/ml [^{3}H]thymidine. CN cells were pulsed-labeled with [^{3}H]thymidine twice with media changes. After a week in test media, CN cells were extracted, and [^{3}H]thymidine incorporation was measured by a Packard 1900CA scintillation counter.

RNA extraction and expression profiling

Neurocytoma specimens were obtained at surgery from three patients; their expression profiles were normalized against those of both ventricular zone tissue and sorted neural progenitors derived from three approximately age-matched samples of freshly resected temporal lobe, taken at epilepsy surgery. RNA was extracted with Trizol (Invitrogen), and then purified using RNeasy (Qiagen, La Jolla, CA), according to the manufacturer's specifications. RNA quality was assessed using either agarose gel electrophoresis or an Agilent Bioanalyzer. A total of 100 ng of total RNA was then amplified using Affymetrix's small sample protocol (GeneChip Eukaryotic Small Sample Target Labeling Technical Note), and 15 μg of cRNA was then hybridized on each U133A GeneChip and scanned according to the manufacturer's instructions (Affymetrix, Santa Clara, CA). Image files were processed using MAS5.0 to produce CHP files. Images were masked to remove streaks/smears present, and no scaling of data was performed during analysis. Data were then imported into GeneSpring (7.2; Silicon Genetics, Redwood City, CA) and per chip normalization performed, using the 50.0th percentile of all measurements in that sample. Gene expression ratios in neurocytoma were calculated by normalization against either the median expression level in adult VZ tissue ($n = 3$) or mean expression level in E/nestin-GFP-sorted progenitors isolated from adult VZ tissue ($n = 2$). An estimate of expression error was generated using the Rocke–Lorenzato global error model (Milliken and Johnson, 1984), which takes into account the variability in the expression level of individual genes, compared with that of the entire data set. As a result, lower and more variably expressed genes are given larger error values, and are thus less likely to be deemed significant using our statistical criteria.

Statistical assignment of differential expression in neurocytoma. The global gene list was initially filtered to remove unreliable data by excluding probe sets, which were not deemed "present" by MAS5.0 in every neurocytoma sample. Transcripts deemed significantly enriched in neu-

rocytoma against either adult VZ tissue or adult nestin-sorted progenitors were calculated from their expression ratios using a two-sample *t* test and Rocke–Lorenzato global error model variances (Milliken and Johnson, 1984). A Benjamini and Hochberg false discovery rate (FDR) of 10% was accepted so as to mitigate the effect of multiple comparisons (Benjamini and Hochberg, 1995).

Annotation of probe sets. Qualifying probe sets for each gene on the Affymetrix Human U133A chip were identified using annotations available from NetAffx (Affymetrix) and Ensembl (www.ensembl.org/human). Annotation and additional data analysis were then performed within an in-house MS Access database.

Real-time RT-PCR. After RNA extraction, amplified cDNA was generated by Ribo-SPIA whole transcriptome amplification (NuGEN Tech, San Carlos, CA). Primers and probes were obtained as Assays-on-Demand from Applied Biosystems (Foster City, CA) (for details, see Table 4). The resulting cDNA was used at 1:20 dilution in three separate real-time PCRs. We used 900 nM forward and reverse primers, and 250 nM FAM-labeled MGB probes. Real-time PCR analysis was performed and the relative abundance of individual transcript expression was calculated by ΔΔCt analysis normalized to 18S RNA. Significance was tested using a two-way, *t* test on $\log_2$ transformed data.

Assessment of IGF2 imprinting

To investigate possible loss of imprinting in the IGF2 gene, IGF2 transcripts were compared with genomic IGF2 as described previously (Ross et al., 1999). Both RNA and genomic DNA (gDNA) were extracted from tumor tissue using Trizol (Invitrogen), and RNA was further purified using Qiagen RNeasy columns with DNase treatment. RNA was reverse transcribed using Superscipt II (Invitrogen), and PCR was performed with LA *Taq* (Takara) on cDNA and gDNA using primers flanking an *Apa*I restriction fragment length polymorphism. Forward primer was as follows: CTTGGACTTTGAGTCAAATTGG. Reverse primer was as follows: CCTCCTTTGGTCTTACTGGG. PCR products were then digested with *Apa*I enzyme (50 U; New England Biolabs, Beverly, MA) overnight at 37°C, separated by electrophoresis on a 4% agarose gel, and visualized using SYBR Gold (Invitrogen). After digestion, individual alleles were visualized as either a single 236 bp fragment or 173 and 63 bp fragments (63 bp was not well resolved).

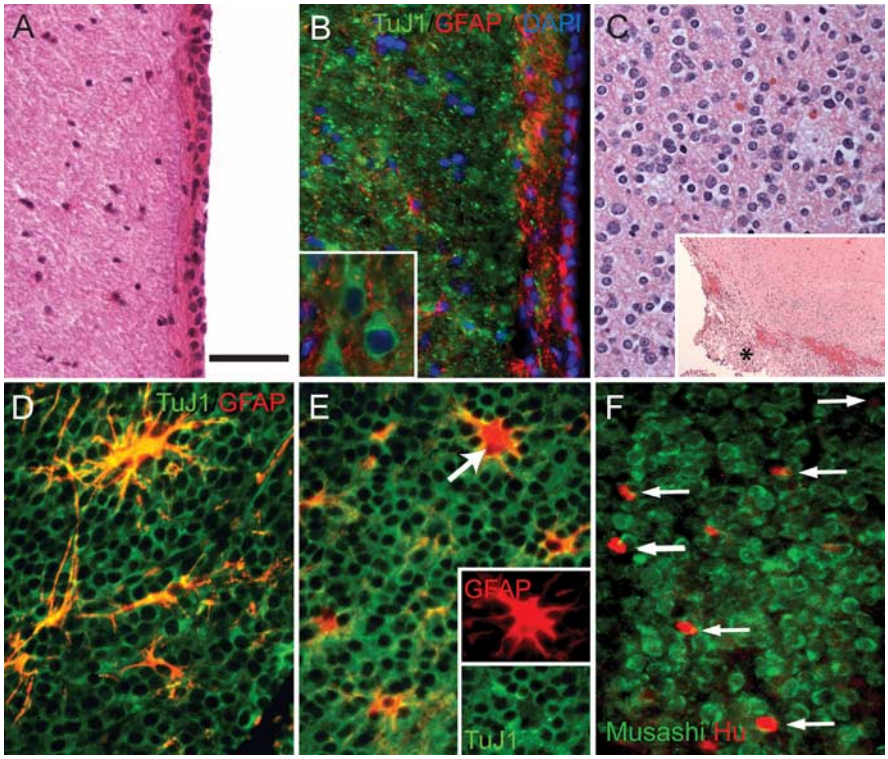

Figure 1. Neurocytoma includes mitotic neuroblasts and a minority of postmitotic neuron-like cells. ***A***, Normal adult human ventricular wall. ***B***, A normal ventricular zone, immunostained for βIII-tubulin/TuJ1 (red), GFAP (green), and DAPI (blue). The normal VZ exhibits a well defined layer of GFAP$^+$ subependymal astrocytes. In contrast to neurocytoma, no TuJ1$^+$ cell bodies were observed adjacent to the ventricular wall in normal tissues, although they were observed in adjacent regions of the same sections (inset shows TuJ1$^+$ hippocampal neurons of this section). ***C***, Histological appearance of neurocytoma (hematoxylin and eosin) (region shown in high-power image indicated by asterisk in inset). ***D–F***, Sections of a central neurocytoma, taken from a 20-year-old male patient with a striatal ventricular wall tumor, immunostained for neuronal βIII-tubulin protein using mAb TuJ1 (green). ***D***, ***E***, GFAP$^+$ astrocytes (red) are scattered among the TuJ1$^+$ cells, which comprise the bulk of the tumor mass (green). GFAP$^+$ cells constituted <5% of the total cell population in each of seven tumors examined. Of note, neurocytoma cells were never noted to coexpress both GFAP and TuJ1. ***F***, The majority of the neurocytoma cells expressed musashi protein, a marker of uncommitted neural progenitor cells (green). Scattered among these were less frequent cells expressing Hu protein (red), a marker of terminally committed and postmitotic neurons. The persistence of Hu$^+$ cells within the musashi$^+$ tumor mass likely represents the generation of postmitotic Hu$^+$ neuronal daughter cells from neoplastic musashi$^+$ progenitor cells. Scale bar, 60 μm.

Results

Neurocytoma exhibits a neuronal progenitor phenotype *in vivo*

Neurocytoma has been previously reported as either a neuronal or mixed neuronal and astrocytic tumor (von Deimling et al., 1991; Maiuri et al., 1995; Ishiuchi and Tamura, 1997). To better define its ontogeny, we immunostained neurocytoma samples derived from a total of 11 patients for a panel of cell-specific proteins, using the normal adult ventricular wall as a point of reference (Fig. 1*A*,*B*). Pathologically, the neurocytoma samples were typical of neurocytoma with a histological appearance similar to that of oligodendroglioma (Fig. 1*C*). The majority of all neurocytoma tumor cells in every sample examined coexpressed both musashi protein, a Notch-regulated marker of uncommitted neural progenitor cells (Imai et al., 2001), and βIII-tubulin and synaptophysin, two early markers of neuronal phenotype (Ishiuchi and Tamura, 1997). Occasional large cells with extensive fiber arrays, expressing GFAP, were also noted scattered about through the tumor (Fig. 1*D*,*E*), but no coexpression of GFAP with either βIII-tubulin or synaptophysin was noted (Fig. 1*D*, inset). In addition, a small proportion of cells within CN tumors, typically <5%, expressed the postmitotic neuronal marker Hu (Fig. 1*F*). Whereas βIII-tubulin expression characterizes premitotic as well as postmitotic neuroblasts (Menezes and Luskin, 1994; Menezes et al., 1995), Hu expression typifies postmitotic neurons (Barami et al., 1995), suggesting that a minor fraction of cells within neurocytoma tumors are postmitotic neuron-like cells generated by neoplastic, musashi$^+$ progenitor cells (Fig. 1*C*). In this regard, we noted no neurofilament heavy-chain immunoreactivity, suggesting that those Hu$^+$ cells generated did not achieve neuronal antigenic maturation or fiber extension within the tumor masses. These observations indicated that neurocytomas are composed predominantly of neuroblasts and their neuronal derivatives, admixed with a minor fraction of GFAP$^+$ cells of astrocytic morphology. Neurocytoma contrasted with the normal cytoarchitecture of the adult human ventricular

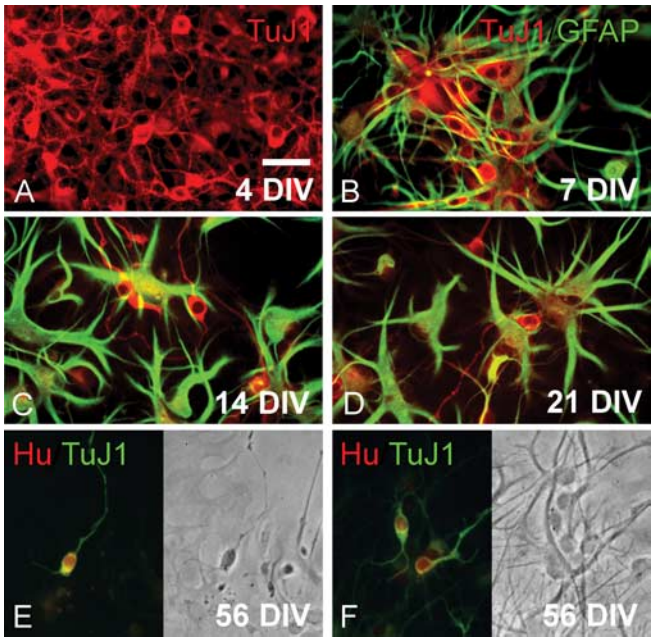

Figure 2. Neurocytoma cells can generate both astrocytes and neuron-like cells in culture. ***A***, βIII-tubulin/TuJ1$^+$ (red) cells of neuronal phenotype, in an unpassaged sample of cultured neurocytoma, after 5 d *in vitro*. ***B–D***, GFAP$^+$ astroglia (green) and TuJ1$^+$ neuroblasts (red), in a second passage culture after 7, 14, and 21 DIV, respectively. Progressive time *in vitro* was accompanied by a relative expansion of astrocytic derivatives. No cells coexpressing GFAP and TuJ1 were ever seen. ***E***, ***F***, A culture double labeled at 56 DIV for TuJ1/βIII-tubulin and Hu, a postmitotic neuronal protein (Barami et al., 1995), revealed that many of the TuJ1$^+$ cells (green) coexpressed Hu (red nuclei), indicating that neurocytoma cells continued to generate neuron-like cells for extended periods of time *in vitro*. Scale bar, 30 μm.

wall, which is comprised of a layer of GFAP$^+$ fibers adjacent to the ependymal layer (Fig. 1*D*). Although TuJ1$^+$ fibers were abundant underlying the GFAP$^+$ layer, no cell bodies were observed.

Neurocytomas give rise to both astrocytic and neuronal progeny *in vitro*

After plating onto monolayers of collagen IV, neurocytoma dissociates were noted to harbor cells of predominantly neuronal, and less so astrocytic, phenotype. Some of the latter expressed GFAP, but >95% of cells expressed neuronal βIII-tubulin (Fig. 2*A*,*B*). Despite the overwhelming predominance of βIII-tubulin$^+$ neuron-like cells after initial plating, within days thereafter we observed the selective expansion of flat, non-neuronal cells (Fig. 2*B–D*). These expressed GFAP, and with repetitive passage preferentially expanded to become the dominant phenotype in culture. No coexpression of neuronal and astrocytic markers was ever noted by single cells. Despite the sustained expansion and rapid predominance of GFAP$^+$ glia in these cultures, βIII-tubulin$^+$/Hu$^+$ neurons were noted to appear in these cultures as long as they were maintained in culture (Fig. 2*D*), in excess of 2 months (see Fig. 4*D*,*E*).

Sustained culture was associated with expansion of a GFAP$^+$ tumor cell

The *in vitro* expansion of neurocytoma cells led rapidly to the selective enrichment of neoplastic GFAP$^+$ cells of astrocytic morphology (Fig. 3*A–F*). These cells exhibited both bizarre and complex morphologies, and divided rapidly *in vitro*. Although the neuron-like cells of the original tumor mass were rapidly diluted during the first several weeks in culture, and most were lost with passage thereafter, neuron-like cells continued to appear during sustained culture (Figs. 2*D*, 3*A–D*). These neuron-like cells were noted to arise from the cells of astroglial morphology, which otherwise expanded to become the dominant phenotype in these cultures. The GFAP$^+$ cells derived from neurocytoma thus appeared to include a persistently neurogenic astroglial progenitor. As such, the neuroblasts of which neurocytoma is mostly comprised *in vivo* could be viewed either as the progeny of a neoplastic, GFAP$^+$ neural stem cell persistent within the tumor mass, or as transit-amplifying progenitors still able to regenerate the parental GFAP$^+$ stem cells from which they themselves may have originated, once removed ex vivo and exposed to a mitogenic environment (Doetsch et al., 2002).

Neurocytoma yielded multipotential neurospheres on repetitive passage

To better assess the lineage and expansion potential of neurocytoma cells, single cells derived from second passage CN cultures were assessed for their ability to generate neurospheres. To this end, we first established the density dependence of CN by serial dilution. When distributed to a 24-well plate at densities of 1000 and 2000 cells · 0.4 ml^{-1} · well^{-1} (2500 and 5000 cells/ml), cell survival was negligible at 1 week, resulting in few or no neurospheres. In contrast, at 4000 cells/0.4 ml (10^4/ml), 459.5 ± 65.3 neurospheres/well (mean ± SD) appeared by 7 days *in vitro* (DIV), suggesting an incidence of clonogenic progenitors of 11.5 ± 1.6% (n = 4 cultures) (Fig. 4*A*). When these primary spheres were re-dissociated to single cells and repassaged, secondary spheres were generated over the following month with similar efficiency (Fig. 4*B*,*C*), suggesting that only a minority of the cells within each expanding neurosphere were serially clonogenic. This in turn suggests that CN cell divisions are asymmetric, with most progeny undergoing terminal differentiation. To assess the differentiated fate of neurocytoma progeny, CN-derived neurospheres were plated onto collagen-coated plates in 10% FBS, and then immunostained 4 d later for βIII-tubulin and GFAP. Whereas the majority of cells emanating from CN neurospheres were GFAP$^+$, βIII-tubulin$^+$ neuron-like cells were noted in abundance within and migrating from all spheres (Fig. 4*D*,*E*). Thus, CN cells can generate passageable neurospheres, which are clonogenic on dissociation and individually multipotential, retaining the capacity to generate neuron-like cells as well as astrocytes.

FGF2 acts as a mitogen for neurocytoma

Both EGF (Reynolds et al., 1992; Reynolds and Weiss, 1992; Morshead et al., 1994; Doetsch et al., 2002) and bFGF (Gensburger et al., 1987; Vescovi et al., 1993; Palmer et al., 1995; Gritti et al., 1996; Pincus et al., 1998b) act as mitogens for neural stem and progenitor cells of the fetal and adult mouse brain. However, in humans, whereas FGF2-dependent signaling has been specifically associated with neural stem cell expansion and neurogenesis (Vescovi et al., 1999; Roy et al., 2000a,b; Arsenijevic et al., 2001; Keyoung et al., 2001), the role of EGF in this regard has been less clear. To assess the potential mitogenic control of neurocytoma, we exposed cultured CN tumor cells to EGF and bFGF, in both serum-free and low-serum media (Ignatova et al., 2002). We saw no effect of EGF on acutely isolated neurocytoma cells (data not shown). In contrast, FGF2 exerted a pronounced mitogenic effect on neurocytoma, with a 140% increase in [^{3}H]thymidine uptake in cultures exposed for 1 week to 40 ng/ml FGF2, compared with unsupplemented cultures (F = 6.41 (1, 6 df); $p < 0.05$, by ANOVA with Bonferroni's *post hoc*). CN cells, like primary hu-

man neural progenitor cells, were thus responsive to the mitogenic effects of bFGF.

Neurocytoma cells activate the early neural enhancer of the nestin gene

Neural stem and progenitor cells may be recognized by their transcriptional activation of the second intronic enhancer of the nestin gene, a sequence that directs neuroepithelial-specific gene expression (Zimmerman et al., 1994; Kawaguchi et al., 2001b). We had previously noted that neural progenitor cells may be identified and sorted from both the mouse and human fetal neuroepithelium, as well as from the adult ventricular wall and hippocampus, based on nestin enhancer-directed, GFP-based FACS (Roy et al., 2000a,b; Wang et al., 2000). On that basis, we asked whether an analogous stage of tumor progenitor might be recognized in neurocytoma by E/nestin-directed GFP expression. To this end, we infected cultured neurocytoma cells with an adenovirus encoding E/nestin:GFP, with the nestin neuroepithelial enhancer placed upstream to an hsp68 basal promoter (Keyoung et al., 2001). Within 2–3 d *in vitro*, abundant GFP$^+$ cells were noted, which expressed GFP under nestin enhancer control (Fig. 4*F*,*G*). When transferred to low-density suspension culture, these cells gave rise to small clusters, which on plating generated both neuron-like cells and astrocytes. Thus, E/nestin:GFP identified multipotential neural progenitor cells in neurocytoma, just as in the fetal and adult ventricular wall (Roy et al., 2000a,b; Kawaguchi et al., 2001a; Keyoung et al., 2001).

Neurocytoma differentially expresses a set of genes associated with neurogenesis

To establish the molecular phenotype of neurocytoma, we assessed the gene expression patterns of three freshly dissected neurocytoma tumors, and compared them with the expression patterns of three non-neoplastic adult human VZ tissue samples, as well as with the expression patterns of isolated VZ neural progenitor cells; the latter were isolated from adult human VZ by E/nestin:GFP-based FACS, as described previously (Roy et al., 2000a). By defining transcripts expressed by neurocytoma cells, but not by non-neoplastic neural progenitor cells or ventricular wall tissue, this normalization strategy was intended to increase the specific identification of genes associated with neurocytoma oncogenesis from native neural progenitors. To this end, we used Affymetrix U133A arrays to compare the gene expression profiles of

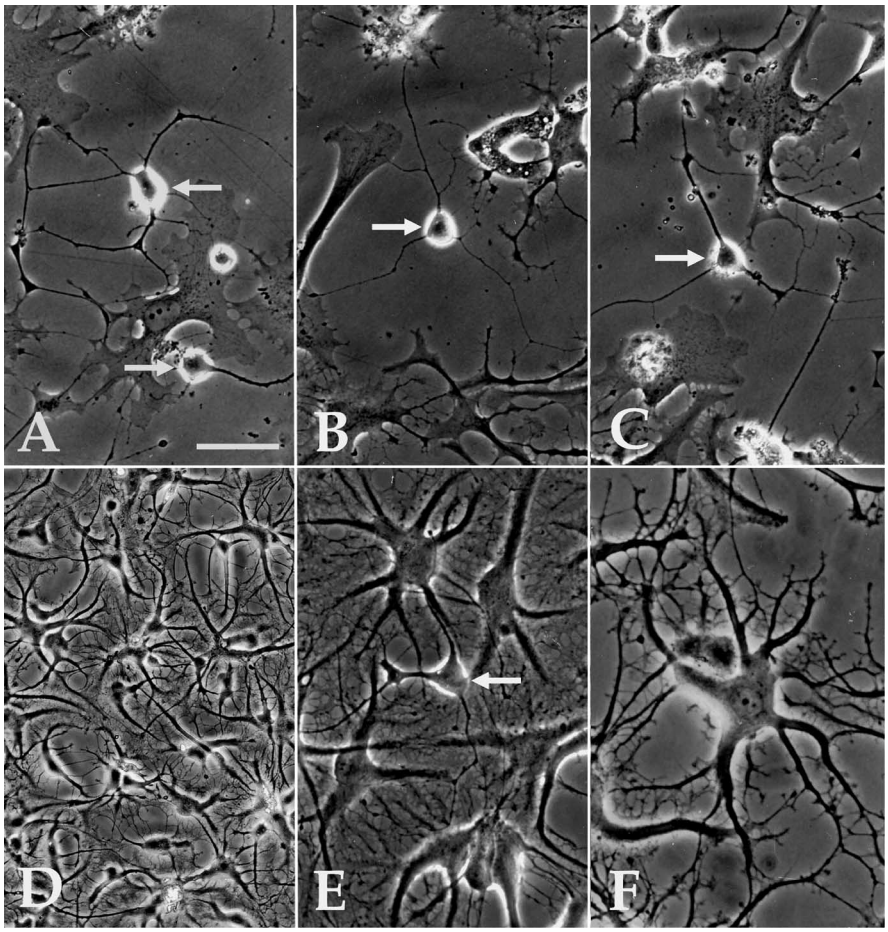

Figure 3. Neurocytoma exhibits selective glial expansion *in vitro*. This neurocytoma was resected from a 20-year-old man, in which it presented as an intraventricular mass arising from the striatal wall. ***A–C***, Neuron-like cells in a monolayer culture of this tumor, after 10 DIV. ***D–F***, Subsequent passage revealed the selective expansion of a glial/progenitor phenotype. The generation of occasional neurons (***E***, arrow) in these cultures suggested their persistent competence as progenitor cells (21 DIV), although their bizarre morphology (***D–F***) suggested their anaplastic transformation. Scale bar, 25 μm.

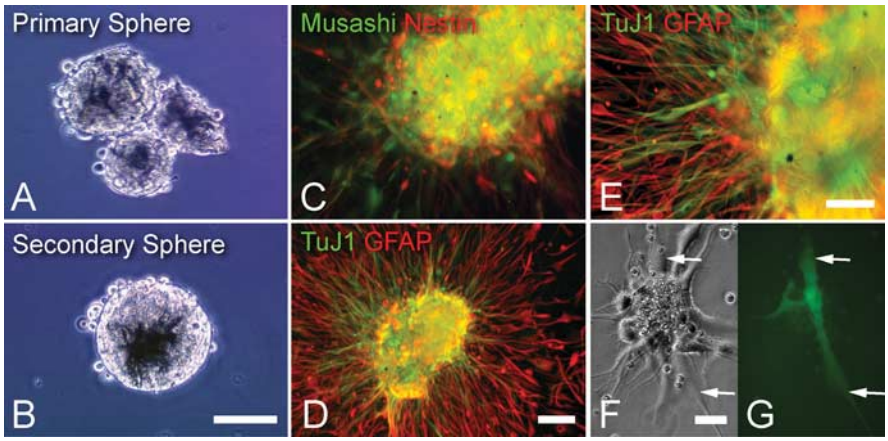

Figure 4. Neurocytoma can generate passageable neurospheres that give rise to neuron-like cells and astrocytes. ***A***, ***B***, Primary (***A***) and secondary (***B***) neurospheres derived from cultured neurocytoma, after monthly passages. ***C***, Neurospheres expressed musashi (green) and nestin (red). ***D***, ***E***, Serial magnifications of secondary neurospheres generated from single CN cells, plated onto collagen to allow the migration of differentiated daughters (2 months *in vitro*). These secondary neurospheres exhibited emigration of both βIII-tubulin$^+$/TuJ1$^+$ neuron-like cells (green) and GFAP$^+$ astrocytes (red). ***F***, ***G***, AdE/nestin:GFP infection revealed a cohort of GFP$^+$ CN cells that transcriptionally activated the neuroepithelial enhancer of the nestin gene. Scale bars: ***A***, ***B***, 60 μm; ***C***, ***E***, 40 μm; ***D***, 75 μm; ***F***, ***G***, 25 μm.

Table 1. Secreted ligands and growth factors overexpressed by neurocytoma

Symbol	Description	Gene ID	Neurocytoma vs adult VZ	Neurocytoma vs adult NSP
LOC492304	IGF2-associated protein	492304	79.99 ± 9.32 ($p=3\times10^{-6}$)	5.17 ± 0.62 ($p=2\times10^{-4}$)
IGF2	Insulin-like growth factor 2	3481	52.36 ± 6.73 ($p=6\times10^{-6}$)	9.36 ± 1.23 ($p=7\times10^{-5}$)
SERPINF1	Serpin PEDF	5176	22.67 ± 11.9 ($p=2\times10^{-3}$)	8.89 ± 4.69 ($p=8\times10^{-3}$)
CXCL12	Chemokine ligand 12 (SCDF1)	6387	15.55 ± 3.77 ($p=3\times10^{-4}$)	3.64 ± 0.90 ($p=5\times10^{-3}$)
JAG1	Jagged1	182	14.34 ± 2.06 ($p=5\times10^{-5}$)	2.84 ± 0.43 ($p=2\times10^{-3}$)
GDF8	Myostatin	2660	13.33 ± 4.86 ($p=1\times10^{-3}$)	27.65 ± 10.1 ($p=6\times10^{-4}$)
PDGFD	Platelet-derived growth factor D	80310	10.76 ± 1.96 ($p=2\times10^{-4}$)	12.13 ± 2.20 ($p=1\times10^{-4}$)
PENK	Proenkephalin	5179	9.43 ± 3.37 ($p=2\times10^{-3}$)	13.30 ± 4.74 ($p=1\times10^{-3}$)
ADCYAP1	PACAP	116	7.88 ± 1.62 ($p=5\times10^{-4}$)	9.32 ± 1.90 ($p=4\times10^{-4}$)
SLIT1	Slit homolog 1 (*Drosophila*)	6585	6.62 ± 0.83 ($p=1\times10^{-4}$)	29.49 ± 3.61 ($p=1\times10^{-5}$)
PCSK2	Subtilisin type convertase 2	5126	5.64 ± 1.33 ($p=2\times10^{-3}$)	16.28 ± 8.44 ($p=3\times10^{-3}$)
NRG2	Neuregulin 2	9542	4.61 ± 0.70 ($p=5\times10^{-4}$)	3.92 ± 0.61 ($p=8\times10^{-4}$)
JMJD1C	Jumonji domain containing 1C	221037	3.10 ± 0.85 ($p=1\times10^{-2}$)	3.70 ± 0.99 ($p=7\times10^{-3}$)
SCG2	Chromogranin C	7857	2.59 ± 0.65 ($p=2\times10^{-2}$)	6.22 ± 1.46 ($p=1\times10^{-3}$)
DBI	Diazepam binding inhibitor	1622	2.08 ± 0.19 ($p=1\times10^{-3}$)	2.02 ± 0.19 ($p=2\times10^{-3}$)

Microarray analysis was performed on total RNA extracted from three neurocytoma tumor resections, and the resulting expression profiles were compared against both normal adult human ventricular zone tissue (adult VZ) and nestin-sorted progenitors (adult NSP) obtained therein. Genes significantly expressed in neurocytoma were identified by *t* test against both adult VZ and adult NSP profiles. The union of those genes was then determined to identify a set of dysregulated genes overexpressed in neurocytoma. From the resulting list of 254 genes, 15 genes were annotated by GO and manual functional annotations as secreted growth factors, proteins, or ligands. This table indicates the ratio of neurocytoma gene expression relative to that of adult VZ or adult NSP; expression ratios are shown with SEs and the two-way *t* test *p* value. All genes reached statistical significance in both comparisons, using a 10% false discovery rate.

neurocytoma samples with those of both sorted human neural progenitor cells, and unsorted normal adult forebrain ventricular zone.

Of a total of >13,000 examined genes, 5425 were detected as present by microarray analysis in all three neurocytoma cases. We then used paired *t* tests and a 10% FDR to generate a set of 835 genes differentially expressed by neurocytoma, relative to normal adult VZ (supplemental Table 1, available at http://www.urmc.rochester.edu/goldmanlab/simkeyoung2006.asp). These CN profiles were also compared with those of adult human VZ cells isolated by E/nestin:GFP-based FACS [referred to as nestin-sorted progenitors (NSPs)]. Using the same paired *t* tests and 10% FDR, we found that 14% of the expressed genes (755 of 5425) were overexpressed in neurocytoma relative to NSPs (supplemental Table 2, available at http://www.urmc.rochester.edu/goldmanlab/simkeyoung2006.asp). The intersection of these two data sets yielded a distinct set of 254 transcripts differentially expressed by CN, relative to both native adult VZ tissue and its derived progenitors (supplemental Fig. 1, available at http://www.urmc.rochester.edu/goldmanlab/simkeyoung2006.asp). Functional classification according to the Gene Ontology (GO) (www.geneontology.org) consortium revealed that neurocytoma overexpressed a set of 20 genes related to neurogenesis (GO:0007399), which included transcripts such as doublecortin (DCX), jagged 1 (JAG1), tailless (NR2E1), dihydropyrimidinase-like 1 and 3 (CRMP1 and DPYSL3), which collectively suggested a mitotically competent, still uncommitted neural progenitor phenotype.

Neurocytoma differentially expressed ligands associated with tumorigenicity

Genes involved in cell proliferation and oncogenesis were expressed at much higher levels in neurocytoma than in both VZ tissue and sorted native progenitor cells. Of special interest were 15 secreted ligands that were highly expressed in CN, relative to both normal ventricular zone and VZ progenitors. The most differentially overexpressed among these were myostatin (GDF8), PDGFD, IGF2, neuregulin 2 (NRG2), and JAG1 (Table 1).

GDF8/myostatin was overexpressed by CN at levels >25- and >10-fold those of nestin-sorted progenitors and adult VZ tissue, respectively. Interestingly, GDF8 and the closely related GDF11 have been shown to promote neuronal differentiation in the olfactory epithelium (Wu et al., 2003). GDF8 binds to both the TGF type II receptor Activin receptor IIB (ActRIIB), and the type I receptor ALK4/5 (Activin receptor-like kinase 4/5), to induce phosphorylation of SMAD2/3 and thereby activate the TGFβ pathway. Furthermore, GDF8 has been shown to specifically block the progliogenic actions of BMP7 (bone morphogenetic protein 7), by binding to ActRIIB (Rebbapragada et al., 2003). GDF8 overexpression may thus contribute to the neuronal differentiation bias of neurocytoma.

The PDGF family member PDGF-D was overexpressed by CN, 12- and 11-fold relative to nestin-sorted progenitors and adult VZ tissue, respectively. Both subependymal and parenchymal glial progenitors express the α and β PDGF receptors, and PDGF-D overexpression has been implicated in the expansion of both astrocytoma and medulloblastoma (LaRochelle et al., 2002). Similarly, NRG2 was also selectively overexpressed by neurocytoma, by fourfold and fivefold relative to sorted progenitors and adult VZ tissue, respectively.

In addition to evidence of excessive GDF8, PDGF, and neuregulin signaling in neurocytoma, we also noted significant overexpression of IGF2. Indeed, IGF2 was the most enriched ligand in neurocytoma, exhibiting >50-fold higher expression relative to the adult VZ, and ~10-fold greater expression than that of the native progenitor pool. The phosphatidylinositol 3′-kinase component p55γ (PIK3R3), a downstream component of IGF2 reception, was also significantly upregulated in CN, whereas other components of the pathway, including phosphatidylinositol 3′-kinase component p85α (PIK3R1), insulin receptor substrate 2 (IRS2), and the IGF-regulated downstream transcriptional regulator FOXO1A, were expressed at higher levels in neurocytoma than nestin-sorted progenitors. These observations were independently validated using real-time RT-PCR of IGF2, p55γ, and IRS2 (see Table 4). IGF2 was significantly differentially expressed >100-fold relative to both NSP and VZ tissue. IRS2 was ~25-fold higher in neurocytoma than NSP, whereas p55γ was >10-fold differentially expressed in neurocytoma versus both NSP and VZ.

In accord with the gene expression data, we found that IGF2 protein was abundantly expressed by both CN-derived neurospheres and histological sections of neurocytoma (Fig. 5*A*,*B*). The marked overexpression of both IGF2 and its downstream signal components strongly suggested that dysregulated autocrine signaling by IGF2 might contribute significantly to the genesis and expansion of neurocytoma. Indeed, in the single infor-

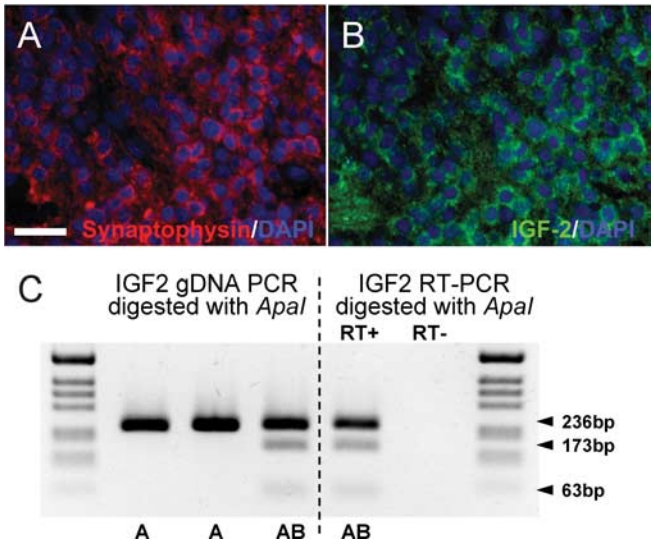

Figure 5. Neurocytoma manifests a loss of imprinting of IGF2 concomitant with IGF2 overexpression. Neurocytoma, immunolabeled for the neuronal marker synaptophysin (red; ***A***), coexpressed IGF-2 (green; ***B***). Virtually all synaptophysin$^+$ neurocytoma cells coexpressed IGF-2. DAPI, 4′,6′-Diamidino-2-phenylindole. ***C***, Southern blotting of neurocytoma genomic DNA coupled with PCR of RNA derived from the same tumor revealed a loss of IGF2 imprinting in the one informative heterozygous case (AB; left). PCR revealed IGF2 transcripts generated from each of the two alleles (right); such a loss of IGF2 imprinting is associated with IGF2 overexpression (Ohlsson, 2004). Scale bar, 40 μm.

mative case heterozygous for IGF2 among the three tumors for which we had available tissue, we observed a frank loss of imprinting, which has been associated with IGF2 overexpression in a variety of tumors (Ohlsson, 2004) (Fig. 5*C*). In that one informative heterozygous case, RT-PCR revealed IGF2 transcripts generated from each of the two alleles identified by PCR on genomic DNA. This biallelic expression indicates a loss of IGF2 imprinting, similar to that which has been noted in other cancers associated with IGF2 overexpression (Zumkeller and Westphal, 2001; Kaneda and Feinberg, 2005; Sakatani et al., 2005).

Neurocytoma differentially expressed receptors associated with stem cell expansion and differentiation

Among the 254 transcripts differentially expressed by neurocytoma relative to both adult ventricular zone and nestin-sorted adult progenitors, Gene Ontology analysis disclosed 35 overexpressed receptors and intracellular signaling components (Table 2). In addition to the overexpressed components of the IGF2 signaling pathway, neurocytoma overexpressed the Wnt coreceptor frizzled-1, as well as the Wnt signaling intermediates TCF4, a transcription factor required for canonical Wnt-dependent gene expression (Fig. 6, Table 3). The expression of both frizzled-1 and TCF4 was confirmed by quantitative PCR (Table 4). Specifically, we confirmed that frizzled-1 was expressed >10-fold higher in neurocytoma than in E/nestin-sorted progenitors [11.2-fold (12.8–9.8); *t* test, $p < 0.01$] and more than fivefold versus VZ tissue [6.7-fold (26.1–7.7); *t* test, $p < 0.05$]. TCF4 (TCF7L2) was expressed at much higher levels in neurocytoma than in either E/nestin-sorted progenitors [14.2-fold (26.1–7.7; $p = 0.08$], or VZ tissue [4.0-fold (5.0–3.1); *t* test, $p < 0.01$].

In addition, neurocytoma overexpressed the nuclear receptors tailless (NR2E1) and retinoid X receptor α (RXRA), each of which has been implicated in neurogenesis. The overexpression by neurocytoma of tailless was of special interest, because tailless contributes to the undifferentiated self-maintenance of neural stem cells (Shi et al., 2004). In addition, CN selectively overexpressed FGFR3, the activity of which has been implicated in progenitor cell differentiation and oligoneogenesis (Bansal et al., 2003).

In addition to these cell genesis-associated receptors, CN selectively overexpressed a number of membrane receptors of note. These included a novel GPCR (G-protein-coupled receptor), GPR1, as well as several transmitter receptors, most notably those for GABA (GABRB1, the $GABA_A$ receptor) and acetylcholine (CHRNA3). The overexpression of the $GABA_A$ receptor by CN cells is of particular note given the newly described role of $GABA_A$ in negatively regulating the postnatal expansion of subventricular zone neural progenitor cells (Liu et al., 2005).

Neurocytoma transcription factors suggested proneuronal transformation

Gene Ontology analysis and manual annotation further revealed 40 transcription factors differentially overexpressed by neurocytoma (Table 3). As noted, the transcription factor TCF4 (TCF7L2), a primary effector of WNT activation, was highly expressed by neurocytoma, as was the wnt receptor FZD1, suggesting the tonic overactivation of canonical WNT signaling in these cells. Yet among all overrepresented transcription factors in neurocytoma, the most differentially expressed compared with adult NSPs was FOXG1B/BF1. This winged helix-loop transcription factor was expressed at levels >300-fold higher in neurocytoma than in native, E/nestin-sorted VZ progenitors. During normal development, BF1 is expressed by telencephalic neuronal progenitors, and modulates both cell cycle and neuronal differentiation (Hanashima et al., 2002), at least in part by interacting with HES1 to repress transcription of bHLH (basic helix-loop-helix) proneural genes (Yao et al., 2001). BF1 overexpression by CN is thus compatible with persistent expression of HES1 by neurocytoma, and would seem likely to contribute to the maintenance of its progenitor phenotype. Moreover, the effects of BF1 and HES1 in supporting progenitor cell renewal may be aided by the relative overexpression of SOX2, SOX4, and SOX11 by neurocytoma. SOX2 in particular has been implicated in neural stem cell maintenance (Zappone et al., 2000) and may act in parallel with HES1 to maintain the progenitor phenotype (Kan et al., 2004; Wegner and Stolt, 2005).

The helix-loop-helix transcription factors nascent helix-loop-helix 1 and 2 (NHLH1 and NHLH2) were also very significantly expressed in neurocytoma, compared with the adult human VZ (22- and 15-fold higher, respectively), and to sorted native progenitors (each >50-fold). Like BF1, both NHLH1 and NHLH2 are expressed in the ventricular zone during embryonic development, but are then downregulated, suggesting that neurocytoma inappropriately recapitulates the transcription factor cascade of the developing VZ (Begley et al., 1992; Gobel et al., 1992).

Discussion

Neurocytoma tumors are relatively homogeneous, including cells almost entirely of neuronal antigenicity. Both *in vivo* and *in vitro*, neurocytoma cells divide and expand to generate proneuronal progeny that express musashi and βIII-tubulin, an expression pattern similar to the neuronally committed transit amplifying progenitors of the adult subependyma. Some mature to express the Hu proteins as markers of postmitotic neurons, although the low incidence of Hu$^+$ cells in neurocytoma suggests that postmitotic neurons generated within these tumors die quickly after their genesis. When removed from the subependymal environment to culture, neurocytoma cells expressed E/nes-

Table 2. Receptors and intracellular signaling components overexpressed in neurocytoma

Symbol	Description	Gene ID	Neurocytoma vs adult VZ	Neurocytoma vs adult NSP
CHRNA3	Cholinergic receptor, nicotinic A3	1136	16.28 ± 2.07 ($p=2\times10^{-5}$)	86.03 ± 21.58 ($p=5\times10^{-5}$)
PLCB4	Phospholipase C, β 4	5332	14.89 ± 4.63 ($p=8\times10^{-4}$)	6.06 ± 1.90 ($p=4\times10^{-3}$)
SCGN	Secretagogin	10590	12.48 ± 8.98 ($p=1\times10^{-2}$)	42.95 ± 30.81 ($p=3\times10^{-3}$)
ARL7	ADP-ribosylation factor-like 7	10123	10.26 ± 0.68 ($p=4\times10^{-6}$)	6.22 ± 0.71 ($p=8\times10^{-5}$)
PIK3R3	PI3 kinase, regulatory unit (p55γ)	8503	8.72 ± 1.94 ($p=5\times10^{-4}$)	6.76 ± 1.51 ($p=9\times10^{-4}$)
ADRA2A	Adrenergic, α -2A-, receptor	150	6.20 ± 1.21 ($p=7\times10^{-4}$)	11.14 ± 2.16 ($p=2\times10^{-4}$)
RGS16	Regulator of G-protein signaling 16	6004	6.00 ± 1.16 ($p=7\times10^{-4}$)	10.23 ± 2.14 ($p=3\times10^{-4}$)
NR2E1	Tailless	7101	5.84 ± 0.91 ($p=3\times10^{-4}$)	276.36 ± 42.04 ($p=3\times10^{-6}$)
ANKRD6	Diversin	22881	5.84 ± 1.45 ($p=2\times10^{-3}$)	17.23 ± 4.25 ($p=3\times10^{-4}$)
KCNA5	K^+ voltage-gated channel, 5	3741	5.48 ± 1.23 ($p=1\times10^{-3}$)	89.17 ± 19.79 ($p=3\times10^{-5}$)
LRP8	Apolipoprotein e receptor	7804	5.36 ± 1.03 ($p=9\times10^{-4}$)	3.41 ± 0.66 ($p=3\times10^{-3}$)
SOCS2	Suppressor of cytokine signaling 2	8835	5.19 ± 1.18 ($p=2\times10^{-3}$)	3.78 ± 0.86 ($p=4\times10^{-3}$)
FGFR3	Fibroblast growth factor receptor 3	2261	4.85 ± 0.82 ($p=7\times10^{-4}$)	912.50 ± 148.72 ($p=2\times10^{-6}$)
PLCL2	Phospholipase C-like 2	23228	4.49 ± 0.91 ($p=2\times10^{-3}$)	6.30 ± 1.25 ($p=7\times10^{-4}$)
RASL11B	RAS-like, family 11, member B	65997	4.46 ± 0.62 ($p=4\times10^{-4}$)	5.52 ± 0.74 ($p=2\times10^{-4}$)
PLCL3	Phospholipase C-like 3	23007	4.27 ± 0.52 ($p=3\times10^{-4}$)	10.37 ± 1.22 ($p=4\times10^{-5}$)
MBIP	MAP3K12 binding inhibitory - 1	51562	4.17 ± 0.88 ($p=2\times10^{-3}$)	4.40 ± 0.92 ($p=2\times10^{-3}$)
FZD1	Frizzled 1	8321	4.09 ± 0.44 ($p=2\times10^{-4}$)	2.41 ± 0.28 ($p=2\times10^{-3}$)
SMAD1	SMAD1	4086	3.97 ± 0.80 ($p=2\times10^{-3}$)	6.16 ± 1.22 ($p=7\times10^{-4}$)
OLFML2B	Olfactomedin-like 2B	25903	3.76 ± 1.00 ($p=6\times10^{-3}$)	5.18 ± 1.35 ($p=3\times10^{-3}$)
RXRA	Retinoid X receptor, α	6256	3.61 ± 0.28 ($p=8\times10^{-5}$)	4.72 ± 0.32 ($p=2\times10^{-5}$)
RASA1	RAS p21 protein activator 1	5921	3.55 ± 0.70 ($p=3\times10^{-3}$)	2.85 ± 0.56 ($p=6\times10^{-3}$)
CCR10	G-protein-coupled receptor 2	2826	3.41 ± 0.29 ($p=1\times10^{-4}$)	3.44 ± 0.28 ($p=1\times10^{-4}$)
AKAP1	A kinase (PRKA) anchor protein 1	8165	3.12 ± 0.31 ($p=3\times10^{-4}$)	6.88 ± 0.83 ($p=8\times10^{-5}$)
GABRB1	$GABA_A$ receptor	2560	3.09 ± 0.18 ($p=4\times10^{-5}$)	106.88 ± 2.06 ($p=2\times10^{-9}$)
AQP6	Aquaporin 6, kidney specific	363	2.99 ± 0.51 ($p=3\times10^{-3}$)	7.65 ± 1.23 ($p=2\times10^{-4}$)
GPR1	G-protein-coupled receptor 1	2825	2.94 ± 0.60 ($p=6\times10^{-3}$)	3.24 ± 0.65 ($p=4\times10^{-3}$)
SH3BP5	SH3-domain binding protein 5	9467	2.70 ± 0.30 ($p=9\times10^{-4}$)	2.07 ± 0.26 ($p=4\times10^{-3}$)
PKIA	Protein kinase inhibitor α	5569	2.59 ± 0.59 ($p=1\times10^{-2}$)	17.95 ± 3.81 ($p=1\times10^{-4}$)
AKAP9	A kinase (PRKA) anchor-9	10142	2.41 ± 0.30 ($p=2\times10^{-3}$)	2.32 ± 0.27 ($p=2\times10^{-3}$)
SLC22A5	Solute carrier family 22–5	6584	2.34 ± 0.30 ($p=3\times10^{-3}$)	3.34 ± 0.37 ($p=4\times10^{-4}$)
NR1D2	Rev-Erb(β)	9975	2.16 ± 0.25 ($p=2\times10^{-3}$)	3.09 ± 0.28 ($p=2\times10^{-4}$)
PPM1A	PP2Cα	5494	2.14 ± 0.21 ($p=1\times10^{-3}$)	3.49 ± 0.25 ($p=6\times10^{-5}$)
CLCN3	Chloride channel 3	1182	2.10 ± 0.35 ($p=1\times10^{-2}$)	3.52 ± 0.59 ($p=2\times10^{-3}$)
THRA	Thyroid hormone receptor, α	7067	1.90 ± 0.24 ($p=7\times10^{-3}$)	9.88 ± 0.89 ($p=1\times10^{-5}$)

Functional annotation using GO and National Center for Biotechnology Information (NCBI) databases, identified a cohort of 35 overexpressed receptor-type genes in the neurocytoma profiles. This list contains cell surface growth factor type, neurotransmitter, and ion channel-type receptors and intracellular signal pathway components. The expression ratio relative to adult VZ or adult NSP are shown with SEs and the two-way *t* test *p* value. All genes reached significance in both comparisons using a 10% false discovery rate.

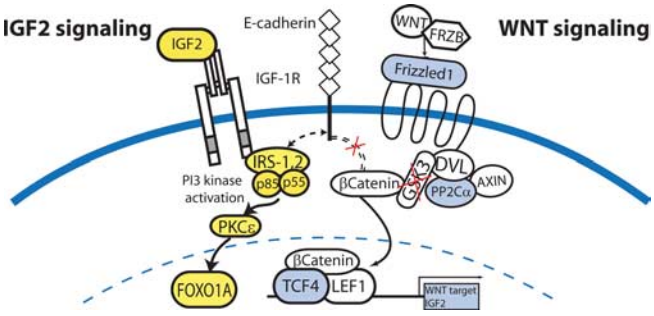

Figure 6. Dysregulated IGF2 signaling in neurocytoma may regulate tumorigenesis. Differentially overexpressed genes in the IGF2 and wnt pathways, noted in yellow and blue, respectively. Our transcriptional analysis suggests that the genesis of CN from native progenitor cells may involve IGF2 overexpression, possibly via loss of imprinting, and excessive IGF2 receptor activation. We hypothesize that the IGF2 signal may cooperate with frizzled3 signaling to potentiate β-catenin translocation and signaling through TCF/LEF.

tin:GFP, divided in response to bFGF, and generated neurospheres, which in turn gave rise to both neurons and astrocytes. The high incidence of neurospheres arising from native neurocytoma cells, >11%, suggested that the dominant musashi$^+$/βIII-tubulin$^+$ proneuronal cells of the neurocytoma were individually capable of regenerating bipotential neuron–astrocyte neural stem cells *in vitro*, in a manner analogous to that of transit amplifying neuronal progenitor cells of the adult subependyma, specifically those designated as type C cells by Alvarez-Buylla and colleagues (Doetsch et al., 2002). Consistent with this hypothesis, we noted that neurocytoma cells expanded *in vitro* principally as a highly fibrous, GFAP$^+$ astroglial phenotype, which within several passages emerged by selective expansion as the predominant phenotype of neurocytoma. These GFAP$^+$ cells assumed extraordinary morphologies *in vitro*, with large and highly fibrous cell bodies; they were remarkably similar in appearance to the few GFAP$^+$ cells noted within the neurocytomas *in vivo*. Notably, cultures of these cells continued to generate apparent postmitotic Hu$^+$ neurons as long as 2 months *in vitro*. Together, these observations suggest that the major phenotype of central neurocytoma may be lineally derived from a GFAP$^+$ cell of astrocytic morphology. The latter may serve as a tumor stem cell, giving rise to proliferative but neuronally committed progeny *in vivo*. However, the neuronal restriction of the latter *in vivo*, and the exquisite environmental regulation of these cells, whose removal to culture was associated with rapid glial differentiation, suggests that central neurocytoma may represent a neoplastic manifestation of transit-amplifying neuronal progenitor cells. In the normal adult brain, the latter derive from GFAP$^+$ subependymal progenitor cells, and can effectively de-differentiate when reexpanded *ex vivo* to regenerate

Table 3. Transcriptional regulators overexpressed by neurocytoma

Symbol	Description	Gene ID	Neurocytoma vs adult VZ tissue	Neurocytoma vs adult NSP
TNRC9	Trinucleotide repeat containing 9	27324	35.43 ± 14.21 ($p=6\times10^{-4}$)	121.59 ± 52.4 ($p=2\times10^{-4}$)
NHLH1	Nescient helix loop helix 1	4807	19.80 ± 4.37 ($p=2\times10^{-4}$)	59.10 ± 13.0 ($p=4\times10^{-5}$)
NHLH2	Nescient helix loop helix 2	4808	14.30 ± 1.59 ($p=2\times10^{-5}$)	53.87 ± 5.95 ($p=3\times10^{-6}$)
SOX4	SRY-box 4	6659	12.59 ± 5.15 ($p=2\times10^{-3}$)	18.39 ± 7.51 ($p=1\times10^{-3}$)
ING1	Inhibitor of growth family, 1	3621	10.71 ± 1.86 ($p=2\times10^{-4}$)	7.42 ± 1.29 ($p=3\times10^{-4}$)
MEIS2	Meis1 and Meis2	4212	7.50 ± 1.02 ($p=1\times10^{-4}$)	46.63 ± 6.21 ($p=8\times10^{-6}$)
TIA1	Cytotoxic granule-RNA BP	7072	5.62 ± 1.47 ($p=2\times10^{-3}$)	3.62 ± 0.74 ($p=3\times10^{-3}$)
SOX11	SRY-box 11	6664	5.35 ± 1.49 ($p=3\times10^{-3}$)	38.48 ± 10.6 ($p=2\times10^{-4}$)
PAX6	Paired box gene 6	5080	4.79 ± 1.55 ($p=7\times10^{-3}$)	217.03 ± 69.1 ($p=5\times10^{-5}$)
NOVA1	Neuro-oncological ventral anti-1	4857	4.60 ± 1.59 ($p=9\times10^{-3}$)	4.63 ± 1.59 ($p=8\times10^{-3}$)
TOX	Thymus high mobility group box	9760	4.24 ± 0.62 ($p=5\times10^{-4}$)	12.25 ± 1.73 ($p=6\times10^{-5}$)
TCF7L2	TCF4	6934	3.80 ± 0.67 ($p=2\times10^{-3}$)	3.59 ± 0.50 ($p=7\times10^{-4}$)
HNRPA0	Nuclear ribonucleoprotein A0	10949	3.77 ± 0.98 ($p=6\times10^{-3}$)	4.71 ± 1.20 ($p=3\times10^{-3}$)
ZHX2	Zinc fingers and homeoboxes 2	22882	3.67 ± 0.59 ($p=1\times10^{-3}$)	5.94 ± 0.92 ($p=3\times10^{-4}$)
SATB1	Special AT-rich seq binding-1	6304	3.58 ± 1.03 ($p=9\times10^{-3}$)	12.93 ± 3.62 ($p=6\times10^{-4}$)
ZBTB20	Zinc finger and BTB domain-20	26137	3.54 ± 0.40 ($p=3\times10^{-4}$)	5.24 ± 0.59 ($p=1\times10^{-4}$)
SMARCA2	SWI/SNF related, A-2	6595	3.52 ± 0.44 ($p=5\times10^{-4}$)	10.26 ± 1.16 ($p=3\times10^{-5}$)
SSBP2	Single-stranded DNA binding-2	23635	3.48 ± 0.82 ($p=5\times10^{-3}$)	2.88 ± 0.67 ($p=9\times10^{-3}$)
BTG1	B cell translocation gene 1	694	3.41 ± 0.37 ($p=3\times10^{-4}$)	2.79 ± 0.30 ($p=6\times10^{-4}$)
FOXG1B	BF1	2290	3.19 ± 0.51 ($p=2\times10^{-3}$)	378.41 ± 56.3 ($p=2\times10^{-6}$)
TCF4	Transcription factor 4	6925	3.15 ± 0.69 ($p=6\times10^{-3}$)	4.05 ± 0.71 ($p=1\times10^{-3}$)
NFIB	Nuclear factor I/B	4781	3.05 ± 0.75 ($p=9\times10^{-3}$)	12.74 ± 3.02 ($p=4\times10^{-4}$)
ZBTB24	Zinc finger and BTB domain - 24	9841	2.93 ± 0.62 ($p=6\times10^{-3}$)	3.10 ± 0.64 ($p=5\times10^{-3}$)
PSIP1	PC4 and SFRS1 interacting-1	11168	2.90 ± 0.38 ($p=1\times10^{-3}$)	6.16 ± 0.73 ($p=1\times10^{-4}$)
PCGF4	BMI1	648	2.87 ± 0.52 ($p=4\times10^{-3}$)	3.20 ± 0.56 ($p=2\times10^{-3}$)
TRIM24	Transcriptional intermediary 1	8805	2.86 ± 0.35 ($p=9\times10^{-4}$)	2.95 ± 0.34 ($p=7\times10^{-4}$)
ZNF91	Zinc finger protein 91	7644	2.71 ± 0.56 ($p=8\times10^{-3}$)	6.82 ± 1.33 ($p=5\times10^{-4}$)
TERF2IP	Telomeric repeat BF2, interacting	54386	2.70 ± 0.47 ($p=4\times10^{-3}$)	5.29 ± 0.86 ($p=5\times10^{-4}$)
BCLAF1	BCL2-associated TF 1	9774	2.56 ± 0.51 ($p=8\times10^{-3}$)	2.51 ± 0.48 ($p=8\times10^{-3}$)
BAZ2B	Bromo and zinc finger domain, 2B	29994	2.52 ± 0.52 ($p=1\times10^{-2}$)	6.17 ± 1.18 ($p=6\times10^{-4}$)
PNN	Pinin, desmosome associated	5411	2.46 ± 0.45 ($p=7\times10^{-3}$)	5.04 ± 0.84 ($p=6\times10^{-4}$)
RBL2	Retinoblastoma-like 2 (p130)	5934	2.38 ± 0.36 ($p=4\times10^{-3}$)	2.25 ± 0.33 ($p=5\times10^{-3}$)
ING3	Inhibitor of growth family - 3	54556	2.36 ± 0.32 ($p=3\times10^{-3}$)	3.58 ± 0.42 ($p=4\times10^{-4}$)
TARDBP	TAR DNA binding protein	23435	2.35 ± 0.39 ($p=6\times10^{-3}$)	3.91 ± 0.59 ($p=8\times10^{-4}$)
ZNF177	Zinc finger protein 177	7730	2.25 ± 0.31 ($p=4\times10^{-3}$)	6.79 ± 0.79 ($p=8\times10^{-5}$)
JMJD2A	Jumonji domain containing 2A	9682	2.24 ± 0.21 ($p=1\times10^{-3}$)	2.32 ± 0.18 ($p=4\times10^{-4}$)
SOX2	SRY-box 2	6657	2.21 ± 0.27 ($p=3\times10^{-3}$)	13.82 ± 1.25 ($p=8\times10^{-6}$)
POLR2K	Polymerase (RNA) II-K	5440	2.13 ± 0.33 ($p=7\times10^{-3}$)	2.33 ± 0.33 ($p=4\times10^{-3}$)
ZNF262	Zinc finger protein 262	9202	2.00 ± 0.20 ($p=2\times10^{-3}$)	2.54 ± 0.33 ($p=2\times10^{-3}$)
ZNF133	Zinc finger protein 133	7692	1.89 ± 0.20 ($p=4\times10^{-3}$)	2.61 ± 0.37 ($p=2\times10^{-3}$)

Regulators of transcription including DNA-binding transcription factors were identified by functional annotation using GO and NCBI databases. Forty distinct transcriptional regulators were identified as overexpressed in neurocytoma. This list includes classic transcription factors, as well as regulators of chromatin structure and telomere function. The expression ratio relative to adult VZ or adult NSP are shown with SEs and the two-way *t* test *p* value. All genes reached significance in both comparisons using a 10% false discovery rate.

Table 4. Real-time RT-PCR validation of IGF2 and WNT pathway components

Expression in neurocytoma	vs nestin-sorted progenitor ($n=2$)	vs normal VZ ($n=3$)	TaqMan assay (Applied Biosystems)
IGF2 pathway			
IGF2	165 (331–82.4; $p<0.01$)	6.3×10^3 (1.0×10^4–3.8×10^3; $p<0.001$)	Hs00171254_m1
IRS2	24.6 (86.0–7.05, ns)	0.50 (1.31–0.19, ns)	Hs00275843_s1
p55γ (PIK3R3)	13.1 (20.6–8.33; ns)	10.9 (13.1–9.04, $p<0.01$)	Hs00300461_s1
WNT pathway			
FZD1	11.2 (12.8–9.8; $p<0.01$)	6.66 (10.1–4.39; $p<0.05$)	Hs00268943_s1
TCF4 (TCF7L2)	14.2 (26.1–7.74; ns)	3.96 (5.03–3.11; $p<0.01$)	Hs00181036_m1

Expression of differentially expressed IGF2 and selected WNT components was validated by real-time RT-PCR analysis. After whole transcriptome ribo-single primer isothermal amplification, and normalization to 18S ribosomal RNA, ΔCt values were compared to control samples (either adult VZ tissue or adult NSP), and significance was assessed by *t* test statistics. After anti-$\log_2$ transformation, mean ratios of expression and ± 1 SE ranges were calculated from ΔΔCt values.

their parental stem cell pool (Doetsch et al., 2002). As such, the transit-amplifying neuronal progenitor cell appears quite similar in its behavior and antigenicity to the predominant phenotype of central neurocytoma.

Mitotic subependymal progenitor cells are distributed widely throughout the ventricular lining of the adult vertebrate forebrain (Morshead et al., 1994; Kirschenbaum and Goldman, 1995; Weiss et al., 1996). These cells are widely distributed throughout the postnatal and adult rodent ventricular systems; analogous progenitors persist in the human forebrain as well (Kirschenbaum et al., 1994; Pincus et al., 1998b; Roy et al., 2000a; Sanai et al., 2004). Yet despite the widespread distribution of progenitors in the adult rat brain, new neurons are actually produced in only a few sites, including the wall of the lateral ventricle, from which new neurons migrate to the olfactory bulb in rodents, and the hippocampus (Goldman, 1998; Gage, 2000, 2002). The restric-

tion of neurogenesis to these few sites reflects the persistence of discrete environmental niches for neurogenesis. The latter appear to be defined and maintained, at the very least, by both local angiogenesis, and active suppression of local bone morphogenetic protein activity by noggin (Lim et al., 2000; Palmer et al., 2000; Louissaint et al., 2002; Chmielnicki et al., 2004). The neuronal restriction of most neurocytoma may therefore reflect the local restriction of tumor daughter cells to neuronal lineage, by virtue of a local imbalance of differentiative cues favoring neuronal ontogeny, or may instead reflect a cell-autonomous program of neuroblastic differentiation. But the multipotentiality of CN cells raised *in vitro*, their ready generation of astrocytes and apparent derivation therefrom, suggest that CN cells indeed remain exquisitely sensitive to their local environment. As such, one may predict the provision of a permissive environment for neurogenesis in the CN ventricular wall.

Our results suggest that neurocytoma derives from a neoplastic GFAP$^+$ cell, which can undergo selective expansion when removed to culture, and which is able to regenerate itself as well as additional neuroblasts. Accordingly, our gene expression data support that central neurocytoma is a tumor of transit-amplifying neuronal progenitor cells. These cells remain environmentally biased to neuronal lineage, and hence may exhibit phenotypic degradation when removed from their subependymal environment. Unfortunately, the rarity of these tumors precluded our acquisition of sufficient live tumor for GFAP-based selection and transplantation, so whether transplanted of isolates of the GFAP$^+$ subpopulation would have been sufficient to transmit the tumor to naive hosts could not be evaluated. That being said, our results strongly suggest the possibility that the neuroblasts that comprise the bulk of cells within central neurocytomas derive from a GFAP$^+$ subependymal progenitor cell, either directly so or by the expansion thereafter of phenotypically restricted neuroblasts derived from that subependymal progenitor.

The close relationship of neurocytoma cells to neural progenitor cells of the adult ventricular zone was apparent in the large proportion of genes whose expression was shared by neurocytoma with both normal ventricular zone and its derived neural progenitor cells. On that basis, the differential expression of a restricted cohort of genes in neurocytoma, relative to the adult VZ, allowed us to define a set of genes potentially involved in the oncogenesis of neurocytoma from native neural progenitor cells. This analysis revealed the potential involvement of a number of dysregulated signaling pathways in neurocytoma. Neurocytoma was especially notable for its differential overexpression of IGF2, especially so when compared with normal adult human ventricular zone cells. IGF2 has been implicated as a primary oncogene in non-neuronal tumors such as Wilm's tumor, in which overexpression leads to oncogenesis via either loss of repression by WT1, or by a loss of genomic imprinting (O'Dell and Day, 1998). In addition, IGF2 overexpression is manifested by other CNS tumors, including periventricular heterotopias and medulloblastoma (Ogino et al., 2001; Hartmann et al., 2005); in the latter, IGF2 overexpression may also result from a patched mutation-associated dysregulation of hedgehog signaling (Hahn et al., 2000). Interestingly, in the single informative heterozygous case that we studied, IGF2 expression failed to manifest imprinting (Fig. 5*C*). Such a loss of IGF2 imprinting has been associated with tumorigenesis in a variety of systems. IGF-1 overexpression has already been associated with increased nuclear translocation of β-catenin, which may in turn support dysregulated growth by affected cells (Playford et al., 2000; Morali et al., 2001). Our data suggest that excessive IGF-2 signaling may have a similarly important role in supporting the genesis and growth of neurocytoma. Moreover, the relative overexpression by neurocytoma of both the Wnt receptor frizzled3 and its nuclear effector TCF4, whose activity is regulated by β-catenin availability, raise the possibility that IGF2 and Wnt/frizzled-dependent signals may cooperate to potentiate neurocytoma tumorigenesis (Fig. 6).

From the therapeutic standpoint, we also noted the selective upregulation of PDGFD and neuregulin ligand expression by neurocytoma. Each of these has been implicated in the genesis of other systemic tumor types, and inhibitory reagents have already been developed for each as clinical antineoplastics. In particular, NRG2 is expressed not only by neural tumors, but also by breast cancers (Dunn et al., 2004), for which therapy aimed at HER2 receptor blockade via the blocking antibody Trastuzumab (Herceptin; Genentech, San Francisco, CA) has already proven efficacious. Similarly, the PDGF receptor is a target of several multifunctional antineoplastics, such as imatinib (Gleevec; Novartis, Basel, Switzerland) and SU11248 (sunitinib malate) (Fiedler et al., 2005), each of which includes the PDGF tyrosine kinase among its principal targets. The identification of these ligands and their cognate pathway components as overexpressed in CN cells suggests their appropriateness as targets for therapeutic suppression not only in neurocytoma but also in the wider set of periventricular tumors of which neurocytoma is representative. Moreover, it is important to note that the identification of these pathways as specifically and differentially active in neurocytoma was made feasible by the direct comparison of neurocytoma gene expression to that of native adult ventricular zone progenitor cells. This direct comparison of the expression profile of a mostly homogeneous tumor phenotype with that of the non-neoplastic progenitor phenotype from which it likely derives, provides us a powerful platform for the discovery of genes causally involved in the neoplastic transformation of tissue-specific stem and progenitor cells.

References

Akimoto J, Itoh H, Itoh Y, Miwa T (1995) Histogenesis of central neurocytoma: an immunohistochemical and electronmicroscopic study of four cases. No Shinkei Geka 23:1083–1091.

Arsenijevic Y, Villemure JG, Brunet JF, Bloch JJ, Deglon N, Kostic C, Zurn A, Aebischer P (2001) Isolation of multipotent neural precursors residing in the cortex of the adult human brain. Exp Neurol 170:48–62.

Bansal R, Lakhina V, Remedios R, Tole S (2003) Expression of FGF receptors 1, 2, 3 in the embryonic and postnatal mouse brain compared with Pdgfralpha, Olig2 and Plp/dm20: implications for oligodendrocyte development. Dev Neurosci 25:83–95.

Barami K, Iversen K, Furneaux H, Goldman SA (1995) Hu protein as an early marker of neuronal phenotypic differentiation by subependymal zone cells of the adult songbird forebrain. J Neurobiol 28:82–101.

Begley CG, Lipkowitz S, Gobel V, Mahon KA, Bertness V, Green AR, Gough NM, Kirsch IR (1992) Molecular characterization of *NSCL*, a gene encoding a helix-loop-helix protein expressed in the developing nervous system. Proc Natl Acad Sci USA 89:38–42.

Benjamini Y, Hochberg Y (1995) Controlling the false discovery rate: a practical and powerful approach to multiple testing. J R Stat Soc 57:289–300.

Chmielnicki E, Benraiss A, Economides AN, Goldman SA (2004) Adenovirally expressed noggin and BDNF cooperate to induce new medium spiny neurons from resident progenitor cells in the adult striatal ventricular zone. J Neurosci 24:2133–2142.

Doetsch F, Petreanu L, Caille I, Garcia-Verdugo JM, Alvarez-Buylla A (2002) EGF converts transit-amplifying neurogenic precursors in the adult brain into multipotent stem cells. Neuron 36:1021–1034.

Dunn M, Sinha P, Campbell R, Blackburn E, Levinson N, Rampaul R, Bates T, Humphreys S, Gullick WJ (2004) Co-expression of neuregulins 1, 2, 3 and 4 in human breast cancer. J Pathol 203:672–680.

Fiedler W, Serve H, Dohner H, Schwittay M, Ottmann OG, O'Farrell AM, Bello CL, Allred R, Manning WC, Cherrington JM, Louie SG, Hong W, Brega NM, Massimini G, Scigalla P, Berdel WE, Hossfeld DK (2005) A phase 1 study of SU11248 in the treatment of patients with refractory or resistent acute myeloid leukemia (AML) or not amenable to conventional therapy for the disease. Blood 105:986–993.

Gage FH (2000) Mammalian neural stem cells. Science 287:1433–1438.

Gage FH (2002) Neurogenesis in the adult brain. J Neurosci 22:612–613.

Gensburger C, Labourdette G, Sensenbrenner M (1987) Brain basic fibroblast growth factor stimulates the proliferation of rat neuronal precursor cells in vitro. FEBS Lett 217:1–5.

Gobel V, Lipkowitz S, Kozak CA, Kirsch IR (1992) NSCL-2: a basic domain helix-loop-helix gene expressed in early neurogenesis. Cell Growth Differ 3:143–148.

Goldman S (2003) Glia as neural progenitor cells. Trends Neurosci 26:590–596.

Goldman SA (1998) Adult neurogenesis: from canaries to the clinic. J Neurobiol 36:267–286.

Gritti A, Parati EA, Cova L, Frolichsthal P, Galli R, Wanke E, Faravelli L, Morassutti DJ, Roisen F, Nickel DD, Vescovi AL (1996) Multipotential stem cells from the adult mouse brain proliferate and self-renew in response to basic fibroblast growth factor. J Neurosci 16:1091–1100.

Hahn H, Wojnowski L, Specht K, Kappler R, Calzada-Wack J, Potter D, Zimmer A, Muller U, Samson E, Quintanilla-Martinez L, Zimmer A (2000) Patched target Igf2 is indispensable for the formation of medulloblastoma and rhabdomyosarcoma. J Biol Chem 275:28341–28344.

Hanashima C, Shen L, Li SC, Lai E (2002) Brain factor-1 controls the proliferation and differentiation of neocortical progenitor cells through independent mechanisms. J Neurosci 22:6526–6536.

Hartmann W, Koch A, Brune H, Waha A, Schuller U, Dani I, Denkhaus D, Langmann W, Bode U, Wiestler OD, Schilling K, Pietsch T (2005) Insulin-like growth factor II is involved in the proliferation control of medulloblastoma and its cerebellar precursor cells. Am J Pathol 166:1153–1162.

Hemmati H, Nakano I, Lazareff J, Masterman M, Geschwind DH, Bronner-Fraser M, Kornblum H (2003) Cancerous stem cells can arise from pediatric brain tumors. Proc Natl Acad Sci USA 100:15178–15183.

Ignatova T, Kukekov V, Laywell E, Suslov O, Vrionis F, Steindler D (2002) Human cortical glial tumors contain neural stem-like cells expressing astroglial and neuronal markers in vitro. Glia 39:193–206.

Imai T, Tokunaga A, Yoshida T, Hashimoto M, Mikoshiba K, Weinmaster G, Nakafuku M, Okano H (2001) The neural RNA-binding protein Musashi1 translationally regulates mammalian numb gene expression by interacting with its mRNA. Mol Cell Biol 21:3888–3900.

Ishiuchi S, Tamura M (1997) Central neurocytoma: an immunohistochemical, ultrastructural and cell culture study. Acta Neuropathol (Berl) 94:425–435.

Ishiuchi S, Nakazato Y, IIino M, Ozawa S, Tamura M, Ohye C (1998) In vitro neuronal and glial production and differentiation of human central neurocytoma cells. J Neurosci Res 51:526–535.

Kan L, Israsena N, Zhang Z, Hu M, Zhao L, Salhni V, Kessler J (2004) Sox1 acts through multiple independent pathways to promote neurogenesis. Dev Biol 269:580–594.

Kaneda A, Feinberg A (2005) Loss of imprinting of IGF2: a common epigenetic modifier of intestinal tumor risk. Cancer Res 65:11236–11240.

Kawaguchi A, Miyata T, Sawamoto K, Takashita N, Murayama A, Akamatsu W, Ogawa M, Okabe M, Tano Y, Goldman SA, Okano H (2001a) Nestin-EGFP transgenic mice: visualization of the self-renewal and multipotency of CNS stem cells. Mol Cell Neurosci 17:259–273.

Keyoung HM, Roy NS, Benraiss A, Louissaint Jr A, Suzuki A, Hashimoto M, Rashbaum WK, Okano H, Goldman SA (2001) High-yield selection and extraction of two promoter-defined phenotypes of neural stem cells from the fetal human brain. Nat Biotechnol 19:843–850.

Kim DG, Paek SH, Kim IH, Chi JG, Jung HW, Han DH, Choi KS, Cho BK (1997) Central neurocytoma—the role of radiation therapy and long term outcome. Cancer 79:1995.

Kirschenbaum B, Goldman SA (1995) Brain-derived neurotrophic factor promotes the survival of neurons arising from the adult rat forebrain subependymal zone. Proc Natl Acad Sci USA 92:210–214.

Kirschenbaum B, Nedergaard M, Preuss A, Barami K, Fraser RA, Goldman SA (1994) In vitro neuronal production and differentiation by precursor cells derived from the adult human forebrain. Cereb Cortex 4:576–589.

LaRochelle WJ, Jeffers M, Corvalan JR, Jia XC, Feng X, Vanegas S, Vickroy JD, Yang XD, Chen F, Gazit G, Mayotte J, Macaluso J, Rittman B, Wu F, Dhanabal M, Herrmann J, Lichenstein HS (2002) Platelet-derived growth factor D: tumorigenicity in mice and dysregulated expression in human cancer 62:2468–2473.

Lee SJ, Kim JE, Paek SH, Keyoung HM, Kim DG, Jung HW (2003) Primary cell culture of central neurocytomas. J Korean Neurosurg Soc 34:238–244.

Lim DA, Tramontin AD, Trevejo JM, Herrera DG, Garcia-Verdugo JM, Alvarez-Buylla A (2000) Noggin antagonizes BMP signaling to create a niche for adult neurogenesis. Neuron 28:713–726.

Liu X, Wang Q, Haydar T, Bordey A (2005) Nonsynaptic GABA signaling in postnatal subventricular zone controls proliferation of GFAP-expressing progenitors. Nat Neurosci 8:1179–1187.

Louissaint Jr A, Rao S, Leventhal C, Goldman SA (2002) Coordinated interaction of neurogenesis and angiogenesis in the adult songbird brain. Neuron 34:945–960.

Maiuri F, Spaziante R, De Caro M, Cappabianca P, Giamundo A, Iaconetta G (1995) Central neurocytoma: a clinicopathological study of 5 cases and review of the literature. Clin Neurol Neurosurg 97:219–228.

Menezes JR, Luskin MB (1994) Expression of neuron-specific tubulin defines a novel population in the proliferative layers of the developing telencephalon. J Neurosci 14:5399–5416.

Menezes JR, Smith CM, Nelson KC, Luskin MB (1995) The division of neuronal progenitor cells during migration in the neonatal mammalian forebrain. Mol Cell Neurosci 6:496–508.

Milliken G, Johnson DK (1984) Analysis of messy data, Vol 1, Designed experiments. Belmont, CA: Wadsworth.

Morali O, Delmas V, Moore R, Jeanney C, Thiery J, Larue L (2001) IGF2 induces rapid βcatenin relocation to the nucleus during epithelium to mesenchyme transition. Oncogene 20:4942–4950.

Morshead CM, Reynolds BA, Craig CG, McBurney MW, Staines WA, Morassutti D, Weiss S, van der Kooy D (1994) Neural stem cells in the adult mammalian forebrain: a relatively quiescent subpopulation of subependymal cells. Neuron 13:1071–1082.

O'Dell SD, Day IN (1998) Insulin-like growth factor II (IGF-II). Int J Biochem Cell Biol 30:767–771.

Ogino S, Kubo S, Abdul-Karim FW, Cohen ML (2001) Comparative immunohistochemical study of insulin-like growth factor II and insulin-like growth factor receptor type 1 in pediatric brain tumors. Pediatr Dev Pathol 4:23–31.

Ohlsson R (2004) Loss of IGF2 imprinting: mechanisms and consequences. Novartis Found Symp 262:108–121.

Palmer TD, Ray J, Gage FH (1995) FGF-2-responsive neuronal progenitors reside in proliferative and quiescent regions of the adult rodent brain. Mol Cell Neurosci 6:474–486.

Palmer TD, Willhoite AR, Gage FH (2000) Vascular niche for adult hippocampal neurogenesis. J Comp Neurol 425:479–494.

Patt S, Schmidt H, Labrakakis C, Weydt P, Fritsch M, CervosNavarro J, Kettenmann H (1996) Human central neurocytoma cells show neuronal physiological properties in vitro. Acta Neuropathol (Berl) 91:209–214.

Pincus DW, Harrison-Restelli C, Barry J, Goodman RR, Fraser RA, Nedergaard M, Goldman SA (1997) In vitro neurogenesis by adult human epileptic temporal neocortex. Clin Neurosurg 44:17–25.

Pincus DW, Keyoung HM, Harrison-Restelli C, Goodman RR, Fraser RA, Edgar M, Sakakibara S, Okano H, Nedergaard M, Goldman SA (1998) Fibroblast growth factor-2/brain-derived neurotrophic factor-associated maturation of new neurons generated from adult human subependymal cells. Ann Neurol 43:576–585.

Playford M, Bicknell D, Bodmer W, Macaulay V (2000) Insulin-like growth factor 1 regulates the location, stability, and transcriptional activity of β-catenin. Proc Natl Acad Sci USA 97:12103–12108.

Rebbapragada A, Benchabane H, Wrana JL, Celeste AJ, Attisano L (2003) Myostatin signals through a transforming growth factor beta-like signaling pathway to block adipogenesis Mol Cell Biol 23:7230–7242.

Reynolds BA, Weiss S (1992) Generation of neurons and astrocytes from isolated cells of the adult mammalian central nervous system. Science 255:1707–1710.

Reynolds BA, Tetzlaff W, Weiss S (1992) A multipotent EGF-responsive

striatal embryonic progenitor cell produces neurons and astrocytes. J Neurosci 12:4565–4574.

Ross J, Schmidt P, Davies S (1999) Genomic imprinting of H19 and insulin-like growth factor-2 in pediatric germ cell tumors. Cancer Cell 85:1389–1394.

Roy NS, Benraiss A, Wang S, Fraser RA, Goodman R, Couldwell WT, Nedergaard M, Kawaguchi A, Okano H, Goldman SA (2000a) Promoter-targeted selection and isolation of neural progenitor cells from the adult human ventricular zone. J Neurosci Res 59:321–331.

Roy NS, Wang S, Jiang L, Kang J, Benraiss A, Harrison-Restelli C, Fraser RA, Couldwell WT, Kawaguchi A, Okano H, Nedergaard M, Goldman SA (2000b) In vitro neurogenesis by progenitor cells isolated from the adult human hippocampus. Nat Med 6:271–277.

Sakatani T, Kaneda A, Iacobuzio-Donahue C, Carter M, Okano H, Ko M, Ohlsson R, Longo D, Feinberg A (2005) Loss of imprinting of IGF2 alters intestinal maturation and tumorigenesis in mice. Science 307:1976–1978.

Sanai N, Tramontin AD, Quinones-Hinojosa A, Barbaro NM, Gupta N, Kunwar S, Lawton MT, McDermott MW, Parsa AT, Manuel-Garcia VJ, Berger MS, Alvarez-Buylla A (2004) Unique astrocyte ribbon in adult human brain contains neural stem cells but lacks chain migration. Nature 427:740–744.

Sanai N, Alvarez-Buylla A, Berger M (2005) Neural stem cells and the origin of gliomas. N Engl J Med 353:811–822.

Schild SE, Scheithauer BW, Haddock MG, Schiff D, Burger PC, Wong WW, Lyons MK (1997) Central neurocytomas. Cancer 79:790–795.

Shi Y, Chichung LD, Taupin P, Nakashima K, Ray J, Yu RT, Gage FH, Evans RM (2004) Expression and function of orphan nuclear receptor TLX in adult neural stem cells. Nature 427:78–83.

Singh S, Clarke I, Terasaki M, Bonn V, Hawkins C, Squire J, Dirks P (2003) Identification of a cancer stem cell in human brain tumors. Cancer Res 63:5821–5828.

Singh S, Hawkins S, Clarke I, Squire J, Bayani J, Hide T, Henkelman M, Cusimano M, Dirks P (2004) Identification of human brain tumor initiating cells. Nature 432:396–401.

Tsuchida T, Matsumoto M, Shirayama Y, Imahori T, Kasai H, Kawamoto K (1996) Neuronal and glial characteristics of central neurocytoma: electron microscopical analysis of two cases. Acta Neuropathol (Berl) 91:573–577.

Vescovi AL, Reynolds BA, Fraser DD, Weiss S (1993) bFGF regulates the proliferative fate of unipotent (neuronal) and bipotent (neuronal/astroglial) EGF-generated CNS progenitor cells. Neuron 11:951–966.

Vescovi AL, Parati EA, Gritti A, Poulin P, Ferrario M, Wanke E, Frolichsthal-Schoeller P, Cova L, Arcellana-Panlilio M, Colombo A, Galli R (1999) Isolation and cloning of multipotential stem cells from the embryonic human CNS and establishment of transplantable human neural stem cell lines by epigenetic stimulation. Exp Neurol 156:71–83.

von Deimling A, Kleihues P, Saremaslani P, Yasargi M, Spoerri O, Sudhof T, Wiestler O (1991) Histogenesis and differentiation potential of central neurocytomas. Lab Invest 64:585–591.

Wang S, Roy NS, Benraiss A, Goldman SA (2000) Promoter-based isolation and fluorescence-activated sorting of mitotic neuronal progenitor cells from the adult mammalian ependymal/subependymal zone. Dev Neurosci 22:167–176.

Wegner M, Stolt C (2005) From stem cells to neurons and glia: a Soxist's view of neural development. Trends Neurosci 28:583–589.

Weiss S, Dunne C, Hewson J, Wohl C, Wheatley M, Peterson AC, Reynolds BA (1996) Multipotent CNS stem cells are present in the adult mammalian spinal cord and ventricular neuroaxis. J Neurosci 16:7599–7609.

Wu HH, Ivkovic S, Murray RC, Jaramillo S, Lyons KM, Johnson JE, Calof AL (2003) Autoregulation of neurogenesis by GDF11. Neuron 37:197–207.

Yao J, Lai E, Stifani S (2001) The winged-helix protein brain factor 1 interacts with groucho and hes proteins to repress transcription. Mol Cell Biol 21:1962–1972.

Zappone MV, Galli R, Catena R, Meani N, De Biasi S, Mattei E, Tiveron C, Vescovi AL, Lovell-Badge R, Ottolenghi S, Nicolis SK (2000) Sox2 regulatory sequences direct expression of a β-geo transgene to telencephalic neural stem cells and precursors of the mouse embryo, revealing regionalization of gene expression in CNS stem cells. Development 127:2367–2382.

Zimmerman L, Parr B, Lendahl U, Cunningham M, McKay R, Gavin B, Mann J, Vassileva G, McMahon A (1994) Independent regulatory elements in the nestin gene direct transgene expression to neural stem cells or muscle precursors. Neuron 12:11–24.

Zumkeller W, Westphal M (2001) The IGF/IGFBP system in CNS malignancy. Mol Pathol 54:227–229.